ChemComm



COMMUNICATION



Cite this: Chem. Commun., 2022, **58**. 12608

Received 6th August 2022, Accepted 19th October 2022

DOI: 10.1039/d2cc04403j

rsc.li/chemcomm

Oxygen-atom transfer photochemistry of a molecular copper bromate complex†

Gerard P. Van Trieste III. Da Joseph H. Reibenspies, Yu-Sheng Chen, b Debabrata Sengupta, Da Richard R. Thompson and David C. Powers *

We report the synthesis and oxygen-atom transfer (OAT) photochemistry of [Cu(tpa)BrO₃]ClO₄. In situ spectroscopy and in crystallo experiments indicate OAT proceeds from a Cu-O fragment generated by sequential Cu-O bond cleavage and OAT from BrOx to [Cu(tpa)]+. These results highlight synthetic opportunities in M-O photochemistry and demonstrate the utility of in crystallo experiments to evaluating photochemical reaction mechanisms.

Reactive ligand-supported metal-oxygen (M-O) species are at the heart of oxygen-atom transfer catalysis in synthesis and biology and have featured prominently in the development of modern theories of metal-ligand (M-L) bonding. As a result, the synthesis and characterization of reactive metal-ligand fragments have garnered significant interest. In the context of Cu-O chemistry, which are responsible for methane hydroxylation in both particulate monooxygenases (pMMOs)1-5 and copper-doped porous materials, enormous synthetic effort has been directed towards the synthesis of molecular site mimics. 6-11 These studies have resulted in the isolation of copper hydroxides, peroxides, hydroperoxides, and superoxides, but the reactivity of terminal Cu-O species has thus far precluded isolation of this structural motif.²

Synthetic photochemistry can enable cryogenic synthesis and thus can enable observation and characterization of species that are otherwise short-lived. To this end, photolysis of metal oxyanion complexes has been explored as a potential source of reactive metal oxygen fragments. In 2015, Zhang and coworkers reported that photolysis of Fe(III) bromate complexes afforded either Fe(IV) or Fe(V) oxo complexes depending on the structure of the supporting porphyrin ligand (Fig. 1a). 12 In related studies of matrix isolated Fe(III) oxyanions complexes,

Suslick and coworkers demonstrated that oxyanion photochemistry was initiated by Fe-O bond homolysis and suggested that subsequent OAT from the extruded radical to the reduced metal center was responsible for oxo complexes observed in steadystate, solution-phase experiments (Fig. 1b). 13-15 In the context of Cu oxyanion chemistry, in 2020 Roithová et al. reported the observation of Cu(tpa)O during collision-induced dissociation mass spectrometry (CID-MS) analysis of [Cu(tpa)OClO₂]⁺ (Fig. 1c). ¹⁶ While this experiment enabled observation of a transient Cu-O species, no spectroscopic or structural data were available.

Here we describe the synthesis, characterization, and OAT photochemistry of copper bromate complex [Cu(tpa)BrO₃]ClO₄ ([8]ClO₄). Steady-state photolysis of [8]ClO₄ results in OAT to carbon monoxide as well as olefinic, benzylic, and aliphatic substrates. Mass spectrometry, in situ spectroscopy, and

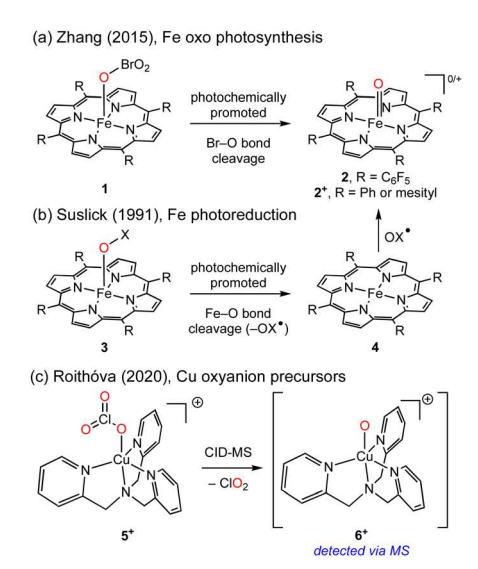


Fig. 1 (a) Ligand-dependent Fe oxo photochemistry of Fe(III) porphyrin bromate complexes. (b) Sequential Fe-O homolysis followed by OAT to the reduced metal fragment could generate M-O species. (c) Collisioninduced disassociation mass spectrometry (CID-MS) observation of Cu-O fragment [6]+

^a Department of Chemistry, Texas A&M University, College Station, Texas 77843, USA. E-mail: powers@chem.tamu.edu

^b ChemMatCARS, University of Chicago, Argonne, IL 60439, USA

[†] Electronic supplementary information (ESI) available: Experimental procedures, spectral data, crystallographic data. CCDC 2178160 and 2178161. For ESI and crystallographic data in CIF or other electronic format see DOI: https://doi. org/10.1039/d2cc04403j

Fig. 2 Synthesis of Cu bromate [8]ClO₄. Displacement ellipsoid plot of [8]ClO₄. H-atoms and counter anions have been omitted for clarity. Ellipsoids drawn at 50% probability. Selected bond lengths (Å): Cu-O = 1.955(3), $Cu-N_{pyridine} = 2.072(4)$, and $Cu-N_{amine} = 2.019(4)$.

in crystallo photochemical experiments are consistent with initial Cu-O bond cleavage to generate [Cu(tpa)]⁺ and BrO₃•. Subsequent OAT from BrO₃ (or BrO obtained by decomposition of BrO₃ to BrO and O₂) to Cu generates a transient Cu-O fragment that is responsible for substrate functionalization. These results provide new entry into reactive Cu-O species and highlight the power of *in crystallo* photochemistry to probe the reactions of molecular inorganic species.

Treatment of [Cu(tpa)Br]ClO₄ ([7]ClO₄) with AgBrO₃ affords [Cu(tpa)BrO₃]ClO₄ ([8]ClO₄) in 65% yield (Fig. 2). The ¹H NMR spectrum of [8]ClO₄ features two paramagnetically shifted peaks at 10 and 29 ppm (Fig. S1, ESI†). The UV-vis spectrum of [8]ClO₄ in acetone displays a weak absorbance centered at 426 (ε = 2.3 \times 10 M⁻¹ cm⁻¹) and stronger absorbances at 710 $(\varepsilon = 3.0 \times 10^2 \text{ M}^{-1} \text{ cm}^{-1})$, and 920 nm $(\varepsilon = 5.4 \times 10^2 \text{ M}^{-1} \text{ cm}^{-1})$ (Fig. S2, ESI†). The IR spectrum of [8]ClO₄ displays spectral features at 831, 842, and 852 cm⁻¹, which are attributed to stretching modes of a Cu-bound bromate ligand (Fig. S3, ESI†).17 Electrospray ionization mass spectrometry (ESI-MS) analysis of [8]ClO₄ displays a signal at m/z = 479.98 with the isotope distribution expected for 8^{+} . Consistent with an S = 1/2 ground state, the X-band EPR spectrum of [8]ClO₄ measured at 4 K features an isotropic signal at g = 2.126(Fig. S4, for X-band EPR spectrum of [7]ClO₄, see Fig. S5, ESI†).

The solid-state structure of [8]ClO₄ is illustrated in Fig. 2 (see Fig. S6 and Table S1 for refinement details, ESI†). The Cu(II) ion in [8]ClO4 is five-coordinate and exhibits a distorted trigonal bipyramidal geometry $(\tau_5 = 0.77)$, with the three pyridine donors from the tpa ligand occupying the equatorial plane. The apical sites are coordinated by the tertiary amine donor of the tpa ligand and an O-bound bromate ligand. The Cu-N distances in [8]ClO₄ (Cu-N_{pyridine} = 2.072(4) Å, Cu-N_{amine} = 2.019(4) Å) are similar to other crystallographically characterized Cu(II)(tpa) complexes and the Cu-O distance (1.955(3) Å) is well-matched to crystallographically characterized Cu(II)(tpa) oxyanion complexes (Table S2, ESI†).

Copper(II) bromate [8]ClO₄ participates in photochemically promoted oxygen-atom transfer (OAT) and hydrogen-atom abstraction (HAA) reactions, which are characteristic of the reactivity patterns of reactive M-O species (Fig. 3). Photolysis ($\lambda > 335$ nm) of a CO-saturated CH₃CN solution of complex [8]ClO₄ afforded CO₂ (detected by GC analysis of the reaction headspace, Fig. S7, ESI†). Similar OAT to olefinic substrates was observed: Photolysis of [8]ClO₄ in the presence of styrene or 1-octene afforded epoxides 9 and 10 in 91% and 36%

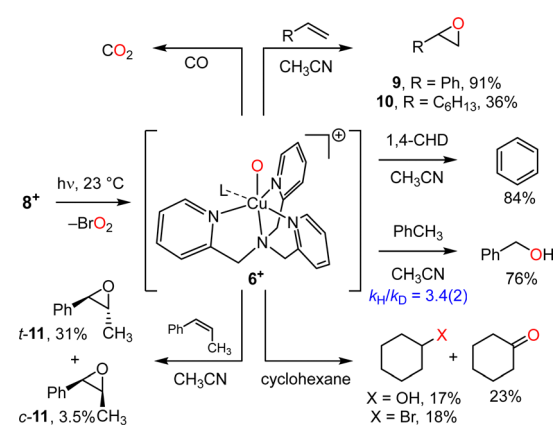


Fig. 3 Summary of photochemically promoted substrate functionalization chemistry. Both OAT and HAA reactivity could arise from a transiently generated reactive CuO fragment (i.e., $[Cu(tpa)(L)O]^+$ (6+)); L = solvent or vacant coordination site.

yields, respectively (Fig. S8 and S9, ESI†). Photolysis in the presence of 1,4-cyclohexadiene (bond dissociation energy (BDE) = 76.0 kcal mol⁻¹)¹⁹ yielded benzene (84% yield), the product of HAA (Fig. S10, ESI†). Photolysis of [8]ClO₄ in toluene $(BDE = 89.7 \text{ kcal mol}^{-1})^{20}$ afforded benzyl alcohol in 76% yield (Fig. S11, ESI†)²¹ and photolysis in the presence of cyclohexane $(BDE = 99.5 \text{ kcal mol}^{-1})^{22}$ afforded a mixture of cyclohexanone (23% yield), cyclohexanol (17% yield), and bromocyclohexane (18% yield) (Fig. S12, ESI†). Photolysis of a CH₃CN solution of [8]ClO₄ in the presence of 1:1 H₈-toluene/D₈-toluene provided a kinetic isotope effect (KIE; k_H/k_D) of 3.4(2) for benzylic hydroxylation, which is consistent with significant C-H cleavage in the rate-determining transition state (Fig. S13, ESI†). Photolysis of [8]ClO₄ in the presence of pentane (BDE = 97.5)²³ or benzene (BDE = 112.9)²⁰ resulted in no observed substrate oxidation. In no case were products of OAT or HAA observed without photolysis (i.e., there are no background reactions with any of the substrates).

To gain additional insight into the mechanism of OAT and the potential intermediacy of [CuO] species (e.g. 6^+), we scrutinized the photochemical epoxidation of stereochemically defined 1,2disubstituted olefins. Epoxidation of cis-β-methylstyrene is not stereospecific: Photolysis of [8]ClO₄ in the presence of cis-βmethylstyrene afforded a 10:1 mixture of trans:cis-11 in 35% yield (Fig. S14, ESI†). For comparison, we also carried out the epoxidation of cis-β-methylstyrene with [Cu(tpa)]BF₄ ([12]BF₄) with PhIO and obtained a 10:1 mixture of trans:cis-11 (Fig. S15, ESI†). The identical stereochemical outcome suggests that both photopromoted and Cu(i) mediated processes proceed via a common intermediate, e.g. a CuO fragment. Taken with the primary KIE observed for benzylic hydroxylation of toluene, these data are consistent with stepwise substrate activation via carbon-centered radicals (i.e., alkyl radicals generated by either radical addition to olefins or via H-atom abstraction (HAA) from alkanes).

In analogy to the oxyanion photochemistry described in Fig. 1, we envisioned that the formation of a [CuO] intermediate could occur via direct photooxidation, i.e., cleavage of the O-Br ChemComm Communication

bond to generate $[Cu(tpa)O]^+$ (6⁺) and BrO₂, or via a photoreduction/OAT sequence, i.e., initial cleavage of the Cu-O bond to generate a [Cu(tpa)]⁺ fragment (12⁺) and BrO₃• following by OAT from BrO₃• (or BrO derived thereof) to 12⁺. A combination of MALDI-MS, in situ spectroscopy data, and in crystallo photochemistry suggest the latter mechanism is operative under steady-state photolysis of [8]ClO₄.

Mass spectrometry data provides evidence for the ions expected from sequential photoreduction and subsequent OAT from BrO₃ to 12+: [Cu(tpa)]+ is the base ion in the MALDI-MS of [8]ClO₄ (indicated by the set of peaks at 353.0 and 355.0 m/z with the expected isotopic distribution) and BrO₃• is detected as BrO₃⁻ via negative-mode MALDI-MS at 126.9 and 128.9 m/z (Fig. 4a inset). OAT from extruded BrO₃ • to [Cu(tpa)]⁺ would be accompanied by the evolution of BrO₂; negative-mode MALDI-MS features at 110.9 and 112.9 m/z correspond to expected isotopic distribution for BrO2. Finally, CID-MS data indicates the formation of Cu-O fragment 6⁺ (Fig. 4). In addition to mass spectrometry, the formation of BrO₂ is also evidence by in situ infrared (IR) spectroscopy: The IR spectrum of Cu bromate [8]ClO₄ in a KBr pellet displays characteristic bromate stretches at 831, 842, and 852 cm⁻¹. Photolysis of this KBr pellet results in the disappearance of

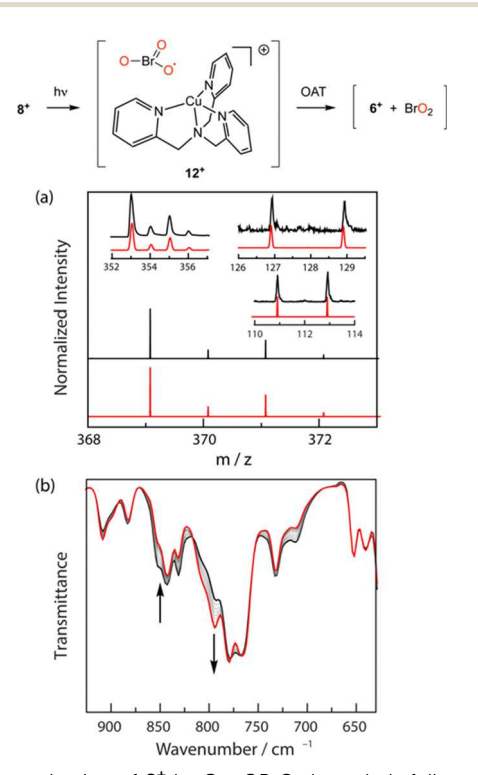


Fig. 4 Photoreduction of 8⁺ by Cu-OBrO₂ homolysis followed by OAT from BrO₃ to 12 would generate 6 and BrO₂. (a) CID-MS analysis shows peaks at 369.1 and 371.1 m/z which correspond to [6]+; MALDI-MS analysis shows peaks at 110.9 and 112.9 m/z which correspond to BrO_2 (black -), simulation (red —) (inset); peaks at 126.9 and 128.9 m/z which correspond to photoextruded BrO_3 (black -), simulation (red -) (inset); and peaks at 353.0 and 355.0 m/z which correspond to [Cu(tpa)]+ (black -), simulation (red —) (inset). (b) IR spectra collected during the photolysis of a KBr pellet of [8]ClO₄ shows a new peak at 795 cm⁻¹, which is attributed to BrO₂.

those spectral features and the evolution of a new peak at 795 cm⁻¹, which is well-matched to a reported stretch for BrO₂ (Fig. 4b).²³ The other stretching mode expected BrO₂ (i.e., 845 cm⁻¹) overlaps with a stretching mode of the [Cu(tpa)]⁺ fragment. Diffuse reflectance and X-band EPR spectra obtained after solid-state photolysis are depicted in Fig. S16 and S17 (ESI†).

Attempts to characterize the photochemistry of [8]ClO₄ by low-temperature solution-phase spectroscopy have been stymied by a combination of insolubility in, or reaction with, common glassy solvents. To avoid these challenges and to build on emerging in crystallo photochemical strategies to characterize reactive species relevant to C-H functionalization, we were attracted to the potential to apply in crystallo photochemistry to directly visualize the primary photochemical events relevant to the OAT chemistry described above. We reasoned that photooxidation via BrO2 loss would be differentiable from initial photoreduction via BrO₃• elimination. To these ends, X-ray diffraction data was collected during 365 nm irradiation of a single crystal of [8]ClO₄ at 100 K using 30 keV synchrotron radiation. Solid-state reaction progress was monitored by free refinement of the Cu-OBrO₂ fragment.

Refinement of the X-ray diffraction data obtained following in crystallo photolysis of [8]ClO₄ are consistent with initial activation of the Cu-O bond (Fig. 5, refinement details collected in Table S3, ESI†). The most significant structural changes induced by photolysis are Cu-O elongation from 1.955(3) Å to 2.22(1) Å and Br-O contraction from 1.657(4) Å (avg.) to 1.53(1) Å (avg.). Accompanying Cu-O elongation, the Cu1-O1-Br1 angle opens from 124.28(2)° to 118.9(5)°. The average O-Br-O angles change minimally from $105.4(2)^{\circ}$ to $103.6(8)^{\circ}$. In contrast to the significant elongation of the Cu-O vector, the Cu-N bonds are not significantly different following photolysis (Fig. 5a). Based on comparison to the metrics of Cu(tpa)Cl, 24 in crystallo photoreduction of [8]ClO₄ to generate BrO₃• and Cu(1) would be anticipated to elongate the Cu-N(4) vector significantly (0.4 Å in [Cu(tpa)Cl]+). Furthermore, the optimized geometry of [Cu(tpa)]⁺, featuring no fifth ligand as would be expected for in crystallo photoreduction, features a Cu-N(4) bond length of 2.2 Å (Table S4, ESI†). As such, the metrics expected for Cu(1) are inconsistent with those observed

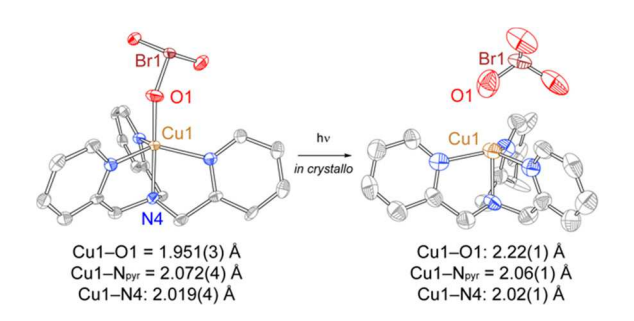


Fig. 5 Displacement ellipsoid plots generated by in crystallo photochemistry of [8]ClO₄. Ellipsoids of [8]ClO₄ are drawn at 50% probability; following photolysis ellipsoids are drawn at 30% probability. H atoms and counter anions are removed for clarity

Communication ChemComm

following in crystallo photolysis. Instead, the observed structural parameters are more consistent with assignment of the in crystallo product of Cu(II)2+ and BrO3-, which could arise from Cu-O homolysis followed by electron transfer (ET) from the initially formed Cu(I) to generate Cu(II). Rapid in crystallo ET may be driven by the dense crystal packing of [8]ClO₄: Unlike previous in crystallo photoreactions in which gaseous, closedshell small molecule leaving groups (e.g. N2 and CO) are extruded from the molecular photoprecursors, 25-29 in crystallo Cu-O cleavage would generate a solid, reactive leaving group (BrO₃•) that is held in proximity to the Cu(1) by virtue of crystal packing (Fig. S18, ESI†).

Finally, we examined the potential that photogenerated BrO₃• was the active oxidant in substrate functionalization chemistry (i.e. reactions pictured in Fig. 3), we evaluated the photochemistry of a mixture of KBrO₃ and (NH₄)₂S₂O₈ in the presence of toluene. Photolysis of a mixture of KBrO3 and (NH₄)₂S₂O₈ has previously been reported to afford BrO₃, which was detected by TA spectroscopy.30 In our experiment, we irradiated a mixture of $KBrO_3$ and $(NH_4)_2S_2O_8$ in acetonitrile with 10 equivalents of toluene added. This reaction afforded a mixture of benzyl alcohol, benzaldehyde, benzoate (Fig. S19, ESI†), which contrasts the selective generation of benzyl alcohol during the photolysis of [8]ClO₄. BrO₃• is known³⁰ to undergo rapid decomposition to BrO and O2 and the control experiment described here does not differentiate between whether OAT to [Cu(tpa)]⁺ is accomplished by BrO3 or reactive oxidants derived thereof. To verify that the observed reactivity is BrO₃ based, and not derived from transient intermediates of (NH₄)₂S₂O₈ photochemistry, we photolyzed a toluene solution of (NH₄)₂S₂O₈ and observed no oxidation products. Control experiments with cyclohexane are described in Fig. S20 (ESI†).

In summary, we report the synthesis and OAT photochemistry of a molecular Cu bromate complex. Photoactivation results in net OAT to CO, olefinic substrates, and C-H bonds to afford CO₂, epoxides, and alcoholic products. In crystallo photochemistry is consistent with initial Cu-O bond cleavage and complementary mass spectrometry and in situ spectroscopy experimental suggest that initial Cu-O homolysis (i.e., photoreduction) precedes the formation of a reactive Cu-O species that is responsible for substrate functionalization. These studies add to a growing body of literature on the prevalence of one-electron photochemistry of metal oxyanion complexes311 and demonstrate new tools to elucidate the atomistic details of molecular photoreactions.

G. P. V. T., D. S., and D. C. P. conceived of the project. G. P. V. T., D. S., and R. R. T. carried out experimental work. All authors participated in data analysis, manuscript writing, and editing.

The authors acknowledge the U.S. Department of Energy (DOE), Office of Science, Office of Basic Energy Sciences, Catalysis Program (DE-SC0018977) and the Welch Foundation (A-1907). Structure determinations were collected at NSF's ChemMatCARS Sector 15, which is supported by NSF/CHE-1834750. Use of the Advanced Photon Source was supported by the U.S. DOE under Contract DE-AC02-06CH11357.

Conflicts of interest

There are no conflicts to declare.

Notes and references

- 1 M. O. Ross, F. MacMillan, J. Wang, A. Nisthal, T. J. Lawton, B. D. Olafson, S. L. Mayo, A. C. Rosenzweig and B. M. Hoffman, Science, 2019, 364, 566.
- 2 R. Davydov, A. E. Herzog, R. J. Jodts, K. D. Karlin and B. M. Hoffman, J. Am. Chem. Soc., 2022, 144, 377.
- 3 G. E. Cutsail, M. O. Ross, A. C. Rosenzweig and S. DeBeer, Chem. Sci., 2021, 12, 6194.
- 4 W. Peng, X. Qu, S. Shaik and B. Wang, Nat. Catal., 2021, 4, 266.
- 5 R. J. Jodts, M. O. Ross, C. W. Koo, P. E. Doan, A. C. Rosenzweig and B. M. Hoffman, J. Am. Chem. Soc., 2021, 143, 15358.
- 6 C. E. Elwell, N. L. Gagnon, B. D. Neisen, D. Dhar, A. D. Spaeth, G. M. Yee and W. B. Tolman, Chem. Rev., 2017, 117, 2059.
- 7 Y. Shimoyama and T. Kojima, Inorg. Chem., 2019, 58, 9517.
- 8 M. Srnec, R. Navrátil, E. Andris, J. Jašík and J. Roithová, Angew. Chem., Int. Ed., 2018, 57, 17053.
- 9 D. Maiti, H. R. Lucas, A. A. Narducci Sarjeant and K. D. Karlin, J. Am. Chem. Soc., 2007, 129, 6998.
- 10 D. Maiti, D.-H. Lee, K. Gaoutchenova, C. Wuertele, M. C. Holthausen, A. A. Narducci Sarjeant, J. Sundermeyer, S. Schindler and K. D. Karlin, Angew. Chem., Int. Ed., 2008, 47, 82.
- 11 S. Hong, S. M. Huber, L. Gagliardi, C. C. Cramer and W. B. Tolman, I. Am. Chem. Soc., 2007, 129, 14190.
- 12 T.-H. Chen, N. Asiri, K. W. Kwong, J. Malone and R. Zhang, Chem. Commun., 2015, 51, 9949.
- 13 D. N. Hendrickson, M. G. Kinnaird and K. S. Suslick, J. Am. Chem. Soc., 1987, 109, 1243.
- 14 K. S. Suslick, J. F. Bautista and R. A. Watson, J. Am. Chem. Soc., 1991,
- 15 K. S. Suslick and R. A. Watson, Inorg. Chem., 1991, 30, 912.
- 16 N. R. M. de Kler and J. Roithova, Chem. Commun., 2020, 56, 12721.
- 17 A. V. Levanov, I. B. Maksimov, O. Y. Isaikina, E. E. Antipenko and V. V. Lunin, Rus. J. Phys. Chem. A, 2016, 90, 1312.
- 18 A. W. Addison, T. N. Rao, J. Reedijk, J. van Rijn and G. C. Verschoor, J. Chem. Soc., Dalton Trans., 1984, 1349.
- 19 Y.-R. Luo, Handbook of Bond Dissociation Energies in Organic Compounds, CRC Press, Boca Raton, 2002.
- 20 S. J. Blanksby and G. B. Ellison, Acc. Chem. Res., 2003, 36, 255.
- 21 Benzyl alcohol is obtained from the analogous photolysis of [8]BF₄, thus perchlorate is not the oxygen source for substrate functionalization.
- 22 L. Bu, P. N. Ciesielski, D. J. Robichaud, S. Kim, R. L. McCormick, T. D. Foust and M. R. Nimlos, J. Phys. Chem. A, 2017, 121, 5475.
- 23 J. Koelm, A. Engdahl, O. Schrems and B. Nelander, Chem. Phys., 1997, 214, 313.
- 24 W. T. Eckenhoff and T. Pintauer, Inorg. Chem., 2007, 46, 5844.
- 25 A. Das, J. H. Reibenspies, Y.-S. Chen and D. C. Powers, J. Am. Chem. Soc., 2017, 139, 2912.
- 26 A. Das, Y.-S. Chen, J. H. Reibenspies and D. C. Powers, J. Am. Chem. Soc., 2019, 141, 16232.
- 27 A. Das, C.-H. Wang, G. P. Van Trieste, C.-J. Sun, Y.-S. Chen, J. H. Reibenspies and D. C. Powers, J. Am. Chem. Soc., 2020, 142, 19862.
- 28 T. Schmidt-Räntsch, H. Verplancke, J. N. Lienert, S. Demeshko, M. Otte, G. P. Van Trieste III, K. A. Reid, J. H. Reibenspies, D. C. Powers, M. C. Holthausen and S. Schneider, Angew. Chem., Int. Ed., 2022, 61, e2021156.
- 29 A. Das, G. P. Van Trieste and D. C. Powers, Comments Inorg. Chem., 2020, 40, 116,
- 30 Z. Zuo and Y. Katsumura, J. Chem. Soc., Farady Trans., 1998, 94, 3577.
- 31 Y. Abderrazak, A. Bhattacharyya and O. Reiser, Angew. Chem., Int. Ed., 2021, 60, 21100.